JACS
JOURNAL OF THE AMERICAN CHEMICAL SOCIETY
Communication
Cite This: J. Am. Chem. Soc. 2017, 139, 14877-14880
pubs.acs.org/JACS

Hard Single-Molecule Magnet Behavior by a Linear Trinuclear Lanthanide–[1]Metallocenophane Complex

Trevor P. Latendresse, Nattamai S. Bhuvanesh, and Michael Nippe*

Department of Chemistry, Texas A&M University, 3255 TAMU, College Station, Texas 77843, United States

Supporting Information

ABSTRACT: A synthetic protocol was developed that involves the transmetalation of a mono-dysprosium–[1]ferrocenophane complex with DyX_3 (X = Cl^- or I^-) to afford $[Dy_3Fc_6Li_2(THF)_2]^-$, featuring a rare linear arrangement of magnetically anisotropic Dy^{3+} ions. The close spatial inter-lanthanide proximity, in combination with μ_2-bridging sp^2-hybridized C_{Cp} groups, enforces significant magnetic coupling and results in hard single-molecule magnet (SMM) behavior, with an effective barrier to magnetization reversal of up to 268 cm^{-1}. Our results highlight the versatility of lanthanide metallocenophane architectures toward the development of novel multinuclear SMM frameworks.

Tunable molecular architectures containing lanthanide ions are being widely studied to drive the discovery of novel complexes for luminescence[1] and magnetism[2] applications, as well as homogeneous catalysis.[3] The development of original ligand platforms that facilitate new functionalities is hereby an important aspect. The large magnetic anisotropy of trivalent lanthanide ions renders them particularly attractive for applications as single-molecule magnets (SMMs).[4] SMMs feature bistable magnetic ground states with thermal barriers (U_{eff}) to magnetization reversal and are potential candidates for high-density data storage[5] and spintronics.[6]

Since the initial discovery of the first lanthanide-based single-ion magnet (SIM) $[Tb(Pc)_2]^-$ (Pc = phthalocyanine),[7] several critical design elements for the generation of high-performance SMMs have been developed[8] and have already led to the directed discovery of SIMs with record barriers and blocking temperatures.[9]

An alternative approach to utilizing discrete single Ln^{3+} ions in SIMs aims at establishing strong magnetic coupling between multiple magnetically anisotropic lanthanide ions in order to reduce quantum-tunneling of the magnetization (QTM) and to create higher spin manifolds in molecular platforms.[10] However, the contracted nature of the lanthanide frontier orbitals typically results in only small magnetic coupling between lanthanide ions. Thus, there is limited precedent for strong intramolecular magnetic coupling between Ln^{3+} ions. Strategically designed ligand bridges such as diffuse open-shell radical moieties[11] and a few closed-shell anionic bridges[12] have been reported to support significant magnetic interactions. A special case in this regard is the report of strong ferromagnetic coupling through phenoxo oxygen ligands in a nearly linear tri-dysprosium SMM, suggesting that linear arrangements of lanthanide ions may enhance the strength of ferromagnetic coupling.[13] We are particularly interested in studying organometallic lanthanide SMMs that feature carbon-based bridging ligands to enhance magnetic interactions. Murugesu et al. had previously reported magnetic studies that include the species shown in Chart 1 and could establish significant ferro- or anti-

Chart 1. (Left) Selected Examples of Multinuclear Lanthanide SMMs Containing C-Bridges and (Right) Structure of New 1 (or 2)

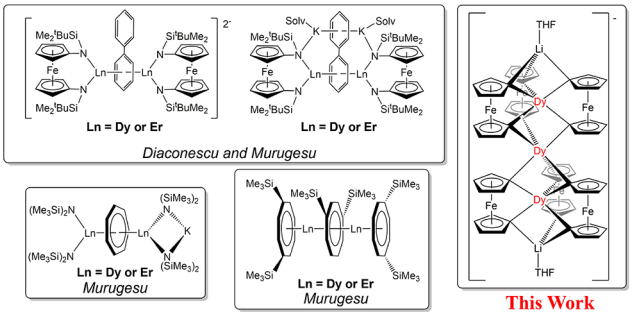

ferromagnetic coupling as well as SMM behavior.[14] While these are fascinating examples of dinuclear SMMs, we argued that closer proximity of the Ln^{3+} ions may lead to even larger magnetic coupling and new dynamic magnetic properties. We report here the first trinuclear linear lanthanide ferrocenophane complexes $[Li_2X(THF)_6][Dy_3Fc_6Li_2(THF)_2]$ (X = I^- (**1**) or Cl^- (**2**)) which display characteristics of very strong magnetic coupling, a significant barrier to magnetization reversal (U_{eff} = 268 cm^{-1} (385 K), and open magnetic hysteresis loops.

We had previously reported[15] that the reaction between $DyCl_3$ and super-stoichiometric amounts of $[Fe(\eta^5\text{-}C_5H_4)_2]_3$-$Li_6(TMEDA)_2$ (TMEDA = tetramethylethylenediamine)[16] results in the formation of $[Li(THF)_4][DyFc_3(THF)_2Li_2]$ (**3**). We subsequently discovered that altering the relative reactant ratios allows for synthetic access to the tri-dysprosium ferrocenophane compounds $[Li_2X(THF)_6][Dy_3Fc_6Li_2(THF)_2]$ (X = I^- (**1**) or Cl^- (**2**)) (Figure 1). We hypothesized that the formation of **1** (or **2**) may involve transmetalation of *in situ*-formed species **3** with a Dy^{3+} salt solvate. In fact, compound **3** can be utilized as a valuable synthon for the clean preparation of **1** (or **2**) (Figure 1). The latter methodology is the preferred route to the isolation of pure **1** (or **2**), as the former *in situ* approach suffers from significant amounts of co-crystallizing **3**.

Received: August 15, 2017
Published: October 12, 2017

DOI: 10.1021/jacs.7b08690
J. Am. Chem. Soc. 2017, 139, 14877–14880

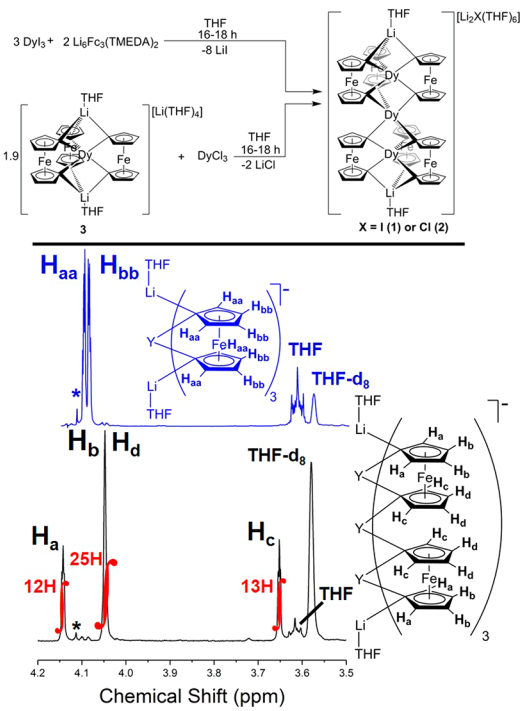

Figure 1. (Top) Synthetic routes to **1** and **2**. (Bottom) ^{1}H NMR (500 MHz, THF-d_8) spectra of diamagnetic mononuclear Y^{3+} ferrocenophane complex (blue)[15] and trinuclear complex **4** (black) with tentative peak assignments. * denotes presence of small amount of ferrocene.

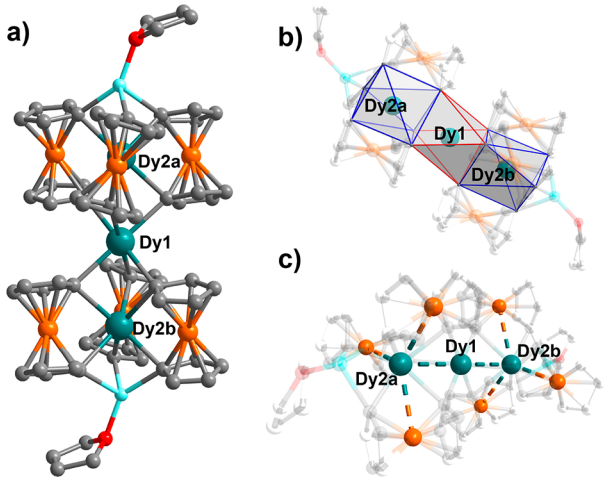

Figure 2. Molecular structure of mono-anionic $[Dy_3Fc_6Li_2(THF)_2]^-$ in crystals of **1** (a). Depiction of approximate octahedral (***Dy1***) and trigonal-prismatic (***Dy2a/b***) coordination spheres (b). View down the trinuclear axis highlighting Dy···Dy and Dy···Fe proximities (c). The countercation, co-crystallized solvent molecules, and hydrogen atoms have been omitted for clarity. Teal, orange, red, gray, and light blue spheres correspond to Dy, Fe, O, C, and Li, respectively.

Diffusion of pentanes into THF solutions of **1** (or **2**) at low temperatures causes the crystallization of **1** (or **2**) as very small, pyrophoric plate crystals with reproducible 13% isolated yields. The small size of crystallites of **1** (or **2**) stands in contrast to the large plate-shaped single crystals readily obtainable for **3** under identical conditions. We additionally investigated if the diamagnetic yttrium analogue[15] of mononuclear compound **3** could also be utilized as a synthon for the preparation of the tri-yttrium analogue of **1** (or **2**). Indeed we find that $[Li_2Cl(THF)_6][Y_3Fc_6Li_2(THF)_2]$ (**4**) can be formed in a similar manner. The ^{1}H NMR spectrum of **4** in THF-d_8 is shown in Figure 1 (for the full spectrum see the Supporting Information (SI), Figure S10) and displays signals that are distinct from those of its mononuclear synthon and are in good agreement with its molecular symmetry.

The molecular structure of **1** (isostructural to **2**; $P\bar{1}$) was established by means of single-crystal X-ray diffraction studies (Figure 2, SI Tables S1 and S2). The structural discussion will be limited to **1**, as X-ray diffraction data were always slightly better for **1** than for **2**. The molecular structure of **1** features three Dy^{3+} ions arranged in a crystallographically enforced linear fashion (angle(***Dy2a–Dy1–Dy2b***) = 180°), in which the central Dy^{3+} ion (***Dy1***) resides on an inversion center and is capped by two crystallographically equivalent $[(THF)LiDyFc_3]^{2-}$ (***Dy2a***, ***Dy2b***) moieties. There is no distortion of the thermal ellipsoid of ***Dy1*** which suggests that the trinuclear axis is in fact linear. The ***Dy1*** ion is formally six coordinate and is surrounded by six C1 atoms of Cp rings, which also allow for bridging between **Dy1** and the upper and lower axial Dy^{3+} ions (***Dy2a*** and ***Dy2b***). We note here, that discrete molecular lanthanide complexes featuring single carbon atom bridges of Cp units are very rare and have previously only been observed for the diamagnetic lanthanide ions Lu^{3+}[17] and La^{3+}.[18] The ligand field geometry around the ***Dy1*** site is best described as distorted octahedral (twist angle ~59°), while the ***Dy2a/b*** sites are best described as distorted trigonal prismatic (twist angle ~19°). A significant asymmetry of the coordination environment of ***Dy2a/b*** is introduced by the combination of Cp-bridging to either a Li^{+} or the larger central Dy^{3+} ion (***Dy1***). Complex **1** features close intramolecular ***Dy1···Dy2a/b*** distances of 3.3598(7) Å. These short contacts place the Dy^{3+} ions well within the range for potential direct magnetic interactions between the spin centers, as intramolecular $Dy^{3+}\cdots Dy^{3+}$ interactions have been measured at distances exceeding 3.4 Å.[19] Similarly to compound **3**, our data suggest that **1** also lacks significant distortions of the ferrocenyl-carbocyclic rings and almost linear $Cp_{Centroid}$–Fe–$Cp_{Centroid}$ bond angles. The average ***Dy2a/b***···Fe distances (3.143[2] Å) observed for compound **1** are even shorter than the Dy···Fe distances reported for mononuclear compound **3** (3.220[4] Å).[15]

The static magnetic properties of **2**, were probed by variable-temperature, direct-current (dc) magnetization measurements in the temperature range of 2–300 K under a 0.1 T applied magnetic field (Figure 3). At room temperature, the value of the molar magnetic susceptibility temperature product ($\chi_M T$) is 43.80 emu·K·mol^{-1}, which is slightly higher but close to the expected value (42.57 emu·K·mol^{-1}) for three non-interacting Dy^{3+} ions (g = 4/3, $^{6}H_{15/2}$, S = 5/2, L = 5). Upon decreasing the temperature, the $\chi_M T$ value gradually increases and at temperatures below 60 K rapidly increases to a maximum value of 96.40 emu·K·mol^{-1} at 7 K below which a sharp decrease to 43.41 emu·K·mol^{-1} is observed. The large increase in $\chi_M T$ at lower temperatures indicates the presence of strong intramolecular ferromagnetic coupling between the three Dy^{3+} ions. Importantly, the field-cooled (FC) and zero-field-cooled (ZFC) magnetization data vary strongly at low temperatures (inset of Figure 3), which suggests blocking of the magnetization by **2**. The temperature at which a maximum of the ZFC magnetization data occurs suggests a blocking temperature (T_B) for **2** of around 4 K and is consistent with the temperature

DOI: 10.1021/jacs.7b08690
J. Am. Chem. Soc. 2017, 139, 14877–14880

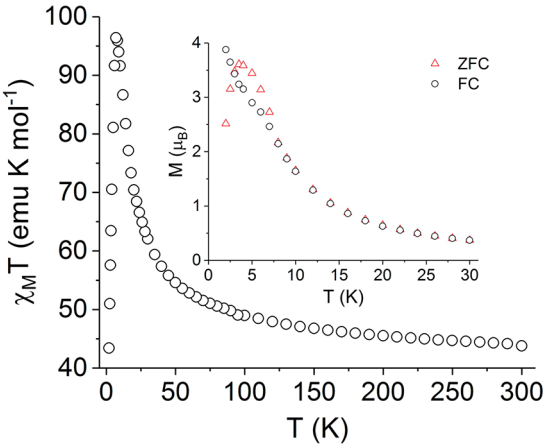

Figure 3. Temperature dependence of $\chi_M T$ for **2**. Inset: Field-cooled (FC) and zero-field-cooled (ZFC) magnetization data for **2**.

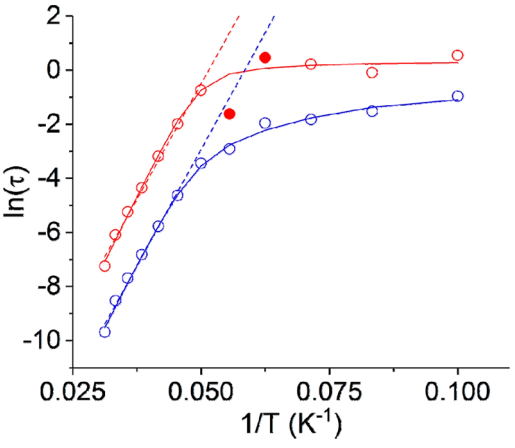

Figure 4. Arrhenius plot for the two relaxation processes (red circle = slow, blue circle = fast) observed for **2** in the temperature range of 10–32 K. Solid lines correspond to fits according to eq 1 (see text), and dashed lined correspond to fits according to $\tau^{-1} = \tau_0^{-1} \exp(-U_{eff}/k_BT)$. Solid circles represent temperatures not included in fitting process.

dependence of the magnetic hysteresis measurements (*vide infra*). Importantly, this temperature is higher than T_B previously reported for mononuclear compound **3** (T_B = 3.5 K). Magnetization (M) data were collected at variable fields at low temperatures, and the corresponding M vs H and M vs H/T curves are provided in the SI, Figures S1 and S2. The non-superimposable M vs H/T curves suggest the expected magnetic anisotropy inherent to **2**. To exclude the possibility of ferromagnetic impurities in crystalline bulk samples of **2**, we also conducted variable-field magnetization measurements at 100 K (SI Figure S3), which showed the expected perfectly linear relationship.

The magnetization dynamics of **2** were probed by variable-temperature alternating-current (ac) magnetometry in the absence of a static dc field. The out-of-phase (χ_M'') and in-phase (χ_M') components of the molar ac magnetic susceptibility over the temperature range from 6 to 34 K is shown in the SI, Figures S4 and S5, respectively. Extending the low-frequency limit of the measurement to 0.1 Hz allowed to observe the beginning of temperature independence of maxima in χ_M'' of compound **2**. This observation suggests that QTM starts to become relevant only at the lowest temperatures and frequencies. The only small presence of QTM in **2** may be a likely result of the above-described significant magnetic coupling between the Dy^{3+} ions in **2**. All temperature-dependent χ_M' and χ_M'' data were used to construct Cole–Cole plots (SI Figure S6). The significant asymmetry of the resulting plots suggests the presence of at least two relaxation processes. Accordingly, two relaxation times (τ) were extracted for each temperature by following previously reported fitting methodologies[20] (corresponding fit parameters are given in the SI, Table S3 and Figures S6–S8). The presence of two magnetic relaxation processes may be ascribed to the presence of the two crystallographically distinct Dy sites in **2** (***Dy1*** and ***Dy2a/b***) or the ability of the spin-coupled system to relax via multiple processes. The thus extracted τ values were used in the construction of Arrhenius plots ($\ln(\tau)$ vs $1/T$; Figure 4), and satisfying fits over the entire temperature range were obtained according to eq 1 (SI Table S4).[21]

$$\tau^{-1} = \tau_{QTM}^{-1} + CT^n + \tau_0^{-1} \exp(-U_{eff}/k_BT) \quad (1)$$

Equation 1 includes contributions from quantum tunneling, Raman scattering, and Orbach processes. For the two relaxation processes we obtained values for U_{eff} of 261 cm^{-1} (376 K) and 268 cm^{-1} (385 K), attempt times (τ_0) of 5.85×10^{-10} and 4.99×10^{-9} s, τ_{QTM} values of 2.35 and 0.736 s, Raman coefficients (C) of 6.83×10^{-6} $s^{-1}\cdot K^{-4.98}$ and 5.90×10^{-7} $s^{-1}\cdot K^{-4.56}$, and Raman exponents (n) of 4.98 and 4.56. The free refinement of the Raman exponent to values close to 5 is in good agreement to a Kramer's ion(s) with low-lying m_J excited states.[21] Fitting solely the linear region of the Arrhenius plot according to $\tau^{-1} = \tau_0^{-1} \exp(-U_{eff}/k_BT)$, we obtained U_{eff} = 240 cm^{-1} (345 K) and 237 cm^{-1} (341 K) and $\tau_0 = 1.72 \times 10^{-9}$ and 2.34×10^{-8} s^{-1}. The U_{eff} values for compound **2** are significantly larger than the previously reported U_{eff} value for mononuclear **3** (108 cm^{-1})[15] and suggests that the magnetic interactions between Dy^{3+} ions may result in an improvement of magnetic properties.

The presence of hysteric behavior in variable-field magnetization data is one crucial property of SMMs. The plethora of reported magnetic hysteresis data of SMMs exhibits waist-restricted or butterfly-like shapes as typically dominant QTM processes result in the loss of remnant magnetization in the absence of a static magnet field. The variable-field magnetization data (0.9 $mT\cdot s^{-1}$) for compound **2** are shown in Figure 5. Importantly, compound **2** displays remnant magnetization at zero field, making it a rare example of a hard SMM. Openings

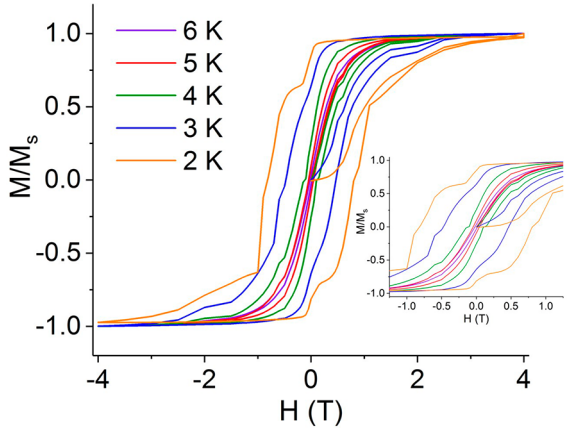

Figure 5. Variable-field magnetization data for **2** collected from 2 to 6 K with a sweep rate of 0.9 $mT\cdot s^{-1}$.

DOI: 10.1021/jacs.7b08690
J. Am. Chem. Soc. 2017, 139, 14877–14880

in magnetic hysteresis curves can be observed up to at least 5 K. These observations contrast the butterfly-shaped hysteresis loops reported for **3** and emphasize the improved magnetic properties of **2** further.

In conclusion, we have shown that mononuclear lanthanide ferrocenophane complexes can be exploited for the targeted preparation of unprecedented linear ferrocenophane-stabilized trinuclear Dy^{3+} complexes in **1** or **2**. The complex magnetic behavior of **2** was investigated and strong ferromagnetic coupling as well as hard SMM behavior of **2** was observed. The origin of the unusually strong ferromagnetic coupling in **2** remains to be elucidated in future investigations. The relative orientations of the magnetic anisotropy axes of the individual Dy^{3+} ions will be an important aspect of these studies. We have performed preliminary calculations using the MAGELLAN software[8b] which suggest a somewhat perpendicular orientation of the anisotropy axes with respect to the trinuclear axis of the molecule (SI Figure S9). We emphasize that these results are based on purely electrostatic considerations (point charges) and that the "true" anisotropy axes are almost certainly differently oriented because of the significant covalent contributions to Dy−C bonding, and future *ab initio* calculations at the CASSCF level will be essential.[22]

This work highlights the value of new ligand frameworks for the generation of advanced SMM architectures. Investigations aimed at the utilization of other magnetically anisotropic lanthanide ions and investigations of redox-tunability of their corresponding magnetic properties are currently ongoing.

■ ASSOCIATED CONTENT

Supporting Information

The Supporting Information is available free of charge on the ACS Publications website at DOI: 10.1021/jacs.7b08690.

Experimental details, additional magnetic data, fit parameters, and crystallographic details (PDF)

X-ray crystallographic data for **1** (CIF)

■ AUTHOR INFORMATION

Corresponding Author

*nippe@chem.tamu.edu

ORCID

Michael Nippe: 0000-0003-1091-4677

Notes

The authors declare no competing financial interest.

■ ACKNOWLEDGMENTS

M.N. is grateful to the TAMU Chemistry Department for generous start-up funds and general financial support by the Welch Foundation (A-1880).

■ REFERENCES

(1) Blackburn, O. A.; Tropiano, M.; Natrajan, L. S.; Kenwright, A. M.; Faulkner, S. *Chem. Commun.* **2016**, *52*, 6111.

(2) Sessoli, R.; Powell, A. K. *Coord. Chem. Rev.* **2009**, *253*, 2328.

(3) Dudnik, A. S.; Weidner, V. L.; Motta, A.; Delferro, M.; Marks, T. J. *Nat. Chem.* **2014**, *6*, 1100.

(4) Woodruff, D. N.; Winpenny, R. E. P; Layfield, R. A. *Chem. Rev.* **2013**, *113*, 5110.

(5) Mannini, M.; Pineider, F.; Sainctavit, P.; Danieli, C.; Otero, E.; Sciancalepore, C.; Talarico, A. M.; Arrio, M. A.; Cornia, A.; Gatteschi, D.; Sessoli, R. *Nat. Mater.* **2009**, *8*, 194.

(6) Mannini, M.; Pineider, F.; Danieli, C.; Totti, F.; Sorace, L.; Sainctavit, P.; Arrio, M. A.; Otero, E.; Joly, L.; Cezar, J. C.; Cornia, A.; Sessoli, R. *Nature* **2010**, *468*, 417.

(7) Ishikawa, N.; Sugita, M.; Ishikawa, T.; Koshihara, S.; Kaizu, Y. *J. Am. Chem. Soc.* **2003**, *125*, 8694.

(8) (a) Rinehart, J. D.; Long, J. R. *Chem. Sci.* **2011**, *2*, 2078. (b) Chilton, N. F.; Collison, D.; McInnes, E. L. J; Winpenny, R. E. P; Soncini, A. *Nat. Commun.* **2013**, *4*, 2551. (c) Chilton, N. F.; Goodwin, C. A. P; Mills, D. P.; Winpenny, R. E. P. *Chem. Commun.* **2015**, *51*, 101.

(9) (a) Guo, F. S.; Day, B. M.; Chen, Y. C.; Tong, M. L.; Mansikkamäki, A.; Layfield, R. A. *Angew. Chem., Int. Ed.* **2017**, *56*, 11445. (b) Goodwin, C. A. P.; Ortu, F.; Reta, D.; Chilton, N. F.; Mills, D. P. *Nature* **2017**, *548*, 439. (c) Ding, Y. S.; Chilton, N. F.; Winpenny, R. E. P.; Zheng, Y. Z. *Angew. Chem., Int. Ed.* **2016**, *55*, 16071. (d) Liu, J.; Chen, Y. C.; Liu, J. L.; Vieru, V.; Ungur, L.; Jia, J. H.; Chibotaru, L. F.; Lan, Y.; Wernsdorfer, W.; Gao, S.; Chen, X. M.; Tong, M. L. *J. Am. Chem. Soc.* **2016**, *138*, 5441. (e) Chen, Y. C.; Liu, J. L.; Ungur, L.; Liu, J.; Li, Q. W.; Wang, L. F.; Ni, Z. P.; Chibotaru, L. F.; Chen, X. M.; Tong, M. L. *J. Am. Chem. Soc.* **2016**, *138*, 2829.

(10) (a) Habib, F.; Murugesu, M. *Chem. Soc. Rev.* **2013**, *42*, 3278. (b) Blagg, R. J.; Ungur, L.; Tuna, F.; Speak, J.; Comar, P.; Collison, D.; Wernsdorfer, W.; McInnes, E. J. L; Chibotaru, L. F.; Winpenny, R. E. P. *Nat. Chem.* **2013**, *5*, 673.

(11) (a) Demir, S.; Jeon, I. R.; Long, J. R.; Harris, T. D. *Coord. Chem. Rev.* **2015**, *289-290*, 149. (b) Rinehart, J. D.; Fang, M.; Evans, W. J.; Long, J. R. *Nat. Chem.* **2011**, *3*, 538. (c) Rinehart, J. D.; Fang, M.; Evans, W. J.; Long, J. R. *J. Am. Chem. Soc.* **2011**, *133*, 14236. (d) Demir, S.; Zadrozny, J. M.; Nippe, M.; Long, J. R. *J. Am. Chem. Soc.* **2012**, *134*, 18546. (e) Gould, C. A.; Darago, L. E.; Gonzalez, M. I.; Demir, S.; Long, J. R. *Angew. Chem., Int. Ed.* **2017**, *56*, 10103. (f) Dolinar, B. S.; Gómez-Coca, S.; Alexandropoulos, D. I.; Dunbar, K. R. *Chem. Commun.* **2017**, *53*, 2283.

(12) (a) Pugh, T.; Vieru, V.; Chibotaru, L. F.; Layfield, R. A. *Chem. Sci.* **2016**, *7*, 2128. (b) Tuna, F.; Smith, C. A.; Bodensteiner, M.; Ungur, L.; Chibotaru, L. F.; McInnes, E. J. L.; Winpenny, R. E. P; Collison, D.; Layfield, R. A. *Angew. Chem., Int. Ed.* **2012**, *51*, 6976.

(13) Hewitt, I. J.; Lan, Y.; Anson, C. E.; Luzon, J.; Sessoli, R.; Powell, A. K. *Chem. Commun.* **2009**, 6765.

(14) (a) Le Roy, J. J.; Jeletic, M.; Gorelsky, S. I.; Korobkov, I.; Ungur, L.; Chibotaru, L. F.; Murugesu, M. *J. Am. Chem. Soc.* **2013**, *135*, 3502. (b) Le Roy, J. J.; Ungur, L.; Korobkov, I.; Chibotaru, L. F.; Murugesu, M. *J. Am. Chem. Soc.* **2014**, *136*, 8003. (c) Huang, W.; Le Roy, J. J.; Khan, S. I.; Ungur, L.; Murugesu, M.; Diaconescu, P. L. *Inorg. Chem.* **2015**, *54*, 2374. (d) Harriman, K. L. M.; Le Roy, J. J.; Ungur, L.; Holmberg, R. J.; Korobkov, I.; Murugesu, M. *Chem. Sci.* **2017**, *8*, 231.

(15) Latendresse, T. P.; Bhuvanesh, N. S.; Nippe, M. *J. Am. Chem. Soc.* **2017**, *139*, 8058.

(16) Perucha, A. S.; Heilmann-Brohl, J.; Bolte, M.; Lerner, H.-W.; Wagner, M. *Organometallics* **2008**, *27*, 6170.

(17) (a) Bauer, T.; Wagner, F. R.; Kempe, R. *Chem. - Eur. J.* **2013**, *19*, 8732. (b) Sobaczynski, A. P.; Bauer, T.; Kempe, R. *Organometallics* **2013**, *32*, 1363. (c) Butovskii, M. V.; Tok, O. L.; Bezugly, V.; Wagner, F. R.; Kempe, R. *Angew. Chem., Int. Ed.* **2011**, *50*, 7695.

(18) Butovskii, M. V.; Döring, C.; Bezugly, V.; Wagner, F. R.; Grin, Y.; Kempe, R. *Nat. Chem.* **2010**, *2*, 741.

(19) Pineda, E. M.; Chilton, N. F.; Marx, R.; Dörfel, M.; Sells, D. O.; Neugebauer, P.; Jiang, S.; Collison, D.; van Slageren, J.; McInnes, E. J. L.; Winpenny, R. E. P. *Nat. Commun.* **2014**, *5*, 5243.

(20) Guo, Y.; Xu, G.; Guo, Y.; Tang, J. *Dalton Trans.* **2011**, *40*, 9953.

(21) Liddle, S. T.; van Slageren, J. *Chem. Soc. Rev.* **2015**, *44*, 6655.

(22) (a) Ungur, L.; Chibotaru, L. F. *Chem. - Eur. J.* **2017**, *23*, 3708. (b) Long, J.; Shestakov, B. G.; Liu, D.; Chibotaru, L. F.; Guari, Y.; Cherkasov, A. V.; Fukin, G. K.; Trifonov, A. A.; Larionova, J. *Chem. Commun.* **2017**, *53*, 4706.

DOI: 10.1021/jacs.7b08690
J. Am. Chem. Soc. 2017, 139, 14877−14880